



2-2014

Peak Power Control of Battery and Super-capacitor Energy Systems in Electric Vehicles

Yash Vardhan Pant

University of Pennsylvania, yashpant@seas.upenn.edu


Truong X Nghiem

University of Pennsylvania, nghiem@seas.upenn.edu

Rahul Mangharam

University of Pennsylvania, rahulm@seas.upenn.edu

Follow this and additional works at: https://repository.upenn.edu/mlab_papers

 Part of the [Computer Engineering Commons](#), and the [Electrical and Computer Engineering Commons](#)

Recommended Citation

Yash Vardhan Pant, Truong X Nghiem, and Rahul Mangharam, "Peak Power Control of Battery and Super-capacitor Energy Systems in Electric Vehicles", . February 2014.

```
@TECHREPORT{TR-2014-ESE01, AUTHOR = {Yash V. Pant and Truong X. Nghiem and Rahul Mangharam}, TITLE = {Peak Power Control of Battery and Super-capacitor Energy Systems in Electric Vehicles}, INSTITUTION = {Department of Electrical and Systems Engineering, University of Pennsylvania}, MONTH = {February}, YEAR = {2014}, }
```

This paper is posted at ScholarlyCommons. https://repository.upenn.edu/mlab_papers/69
For more information, please contact repository@pobox.upenn.edu.

Peak Power Control of Battery and Super-capacitor Energy Systems in Electric Vehicles

Abstract

Hybrid energy systems consist of a load powered by a source and a form of energy storage. Systems with mixed energy supply find applications in the electric grid with renewable and non-renewable sources, in mission critical systems such as Mars rovers with rechargeable and non-rechargeable batteries and low-power monitoring systems with energy harvesting. A general problem for hybrid energy systems is the reduction of peak power consumption to ensure cost-efficient operation as peak power draws require additional resources, adversely affect the system reliability and storage lifetime. Furthermore, in some cases such as electric vehicles, the load dynamics are fast, not perfectly known a priori and the computation power available is often limited, making the implementation of traditional optimal control difficult. This paper aims to develop a control scheme to reduce the peak power drawn from the source for hybrid energy systems with limited computation power and limited load forecasts. We propose a scheme with two control levels and provide a sufficient condition for control of the different energy storage/generation components to meet the instantaneous load while satisfying a peak power threshold. The scheme provides performance comparable to Model Predictive Control, while requiring less computation power and only coarse-grained load predictions. As a case study we implement the scheme for a battery-supercapacitor system in an electric vehicle with real world drive cycles to demonstrate the low execution time and effective reduction of the battery power (hence temperature), which is crucial to the lifetime of the battery.

Keywords

Peak power reduction, hybrid energy storage systems, electric vehicles

Disciplines

Computer Engineering | Electrical and Computer Engineering

Comments

@TECHREPORT{TR-2014-ESE01, AUTHOR = {Yash V. Pant and Truong X. Nghiem and Rahul Mangharam}, TITLE = {Peak Power Control of Battery and Super-capacitor Energy Systems in Electric Vehicles}, INSTITUTION = {Department of Electrical and Systems Engineering, University of Pennsylvania}, MONTH = {February}, YEAR = {2014}, }

Peak Power Control of Battery and Super-capacitor Energy Systems in Electric Vehicles

Yash V. Pant, Truong X. Nghiem and Rahul Mangharam

Department of Electrical and Systems Engineering

University of Pennsylvania

{yashpant, nghiem, rahul}@seas.upenn.edu

Abstract—Hybrid energy systems consist of a load powered by a source and a form of energy storage. Systems with mixed energy supply find applications in the electric grid with renewable and non-renewable sources, in mission critical systems such as Mars rovers with rechargeable and non-rechargeable batteries and low-power monitoring systems with energy harvesting. A general problem for hybrid energy systems is the reduction of peak power consumption to ensure cost-efficient operation as peak power draws require additional resources, adversely affect the system reliability and storage lifetime. Furthermore, in some cases such as electric vehicles, the load dynamics are fast, not perfectly known *a priori* and the computation power available is often limited, making the implementation of traditional optimal control difficult. This paper aims to develop a control scheme to reduce the peak power drawn from the source for hybrid energy systems with limited computation power and limited load forecasts. We propose a scheme with two control levels and provide a sufficient condition for control of the different energy storage/generation components to meet the instantaneous load while satisfying a peak power threshold. The scheme provides performance comparable to Model Predictive Control, while requiring less computation power and only coarse-grained load predictions. As a case study we implement the scheme for a battery-supercapacitor system in an electric vehicle with real world drive cycles to demonstrate the low execution time and effective reduction of the battery power (hence temperature), which is crucial to the lifetime of the battery.

I. INTRODUCTION

Hybrid energy systems (HES) consist of a load powered by a source and a renewable form of energy storage. They find use in many applications due to their unique properties (e.g., fast response time, peak power reduction, supplementary energy source) and the potential advantages (e.g., cost-efficient operation, longer battery lifetimes) they offer over homogeneous energy systems. A common problem across different HES is peak power demands which result in cost intensive operation, increased capacity requirements, faster degradation of energy storage resources and potentially lower reliability of the energy delivery system. For example, in the electric grid, peak power demands are costly as they require additional (usually inefficient) backup power plants to be switched on to meet the demand, raising the operating cost [1]. In the case of battery driven systems like electric vehicles, peak power demands have an adverse effect on battery lifetime [2].

This work was supported in part by TerraSwarm, one of six centers of STARnet, a Semiconductor Research Corporation program sponsored by MARCO and DARPA and also by the US Department of Transportation University Transportation Center Program.

Smart control of how to use a combination of a power source and a renewable energy storage (or generation) in HES can lead to peak power reduction on the energy source. The problem of peak power reduction with HES has been studied for many systems [3], [4], [5] including electric vehicles, where the use of supercapacitors to reduce power demands on batteries has been a well studied topic [6].

To solve the peak power problem for HES, our main contributions in this paper are: a) we propose a scheme which has two levels of control: a simple low-level control algorithm running at a fast sampling rate to directly actuate the plant; and a more complex high-level control algorithm running at a slow sampling rate to compute optimal parameters for the low-level control to operate under a peak threshold. This architecture makes the scheme suitable for systems with fast dynamics because all the complex computations are not affected by the low-level sampling rate. b) The scheme does not require fine grained load predictions at every time step. c) We provide a sufficient condition for controlling different energy sources to meet the instantaneous load while satisfying a peak power threshold and energy constraints on the HES. The proposed control scheme operates with good performance while being computationally efficient, which lends itself to an online implementation.

A. The hybrid energy system model

We consider a HES consisting of three components: a **load**, a **power source** and an **energy storage**. An example of a HES is shown in Fig. 1. The load has an instantaneous energy demand at every time $t \geq 0$, denoted $d(t)$, that needs to be supplied exactly. Examples of loads are electric appliances in a building, and electric motors in an electric vehicle (EV). Typically d is non-negative, which means that energy needs to be supplied to the load. However, in certain applications such as EVs, d can be negative, which means the load has regeneration energy that can be used by the other components.

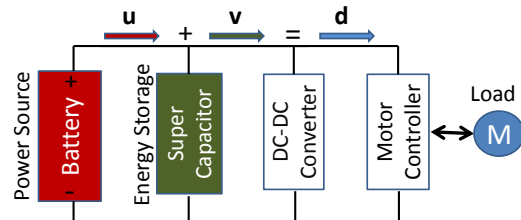


Fig. 1. A simplified view of an architecture for a battery and supercapacitor hybrid energy source powering an EV motor.

The power source, or source for short, is the main energy supplier in the system, e.g., the electric grid for buildings and the battery in an EV. The source has high energy density and can provide a large amount of energy over time. However, as discussed earlier, it is desirable to avoid high peaks in the power drawn from the source. Let $u(t)$ denote the power rate of the source at time t , which is positive (negative) if power flows out of (into) the source.

The energy storage, or storage for short, has the capability to store short-term energy, e.g., supercapacitors. It is used to alleviate the peak power issues by reducing, or flattening, the power drawn from the source. Similar to the source, $v(t)$, which denotes the power rate of the storage at time t , is positive (negative) if power flows out of (into) the storage. The state of charge (SoC) of the storage is denoted by x . Because of its limited capability to store energy, x is constrained between a minimum value x_{\min} and a maximum value x_{\max} , where $x_{\min} < x_{\max}$. When $x = x_{\min}$, the storage is fully discharged, or exhausted. When $x = x_{\max}$, the storage is fully charged. We assume an ideal storage with no charge and discharge losses, therefore its SoC has a simple first-order dynamics: $\frac{dx(t)}{dt} = -v(t)$ with saturations at x_{\min} and x_{\max} .

The relation between the three components is specified by a balance equation which states that at any time t , the load's demand must be matched by the source and the storage:

$$u(t) + v(t) = d(t), \quad \forall t \geq 0. \quad (1)$$

B. Organization of the paper

The rest of this paper is organized as follows. Section II discusses the standard predictive control approach and its limitations. In Section III we introduce the basic idea and structure of our control scheme, and a key theorem that is central to the scheme. In Section IV we present the high-level control optimization of the scheme. An adaptive thresholding algorithm for a finer time scale is discussed in Section IV-D. Section V consolidates the previous sections and highlights the overall detailed structure of the proposed scheme. We evaluate our scheme when applied to a battery-supercapacitor system on a EV and compare it to other schemes to show its benefits in Section VI. Finally, in Section VII we conclude and discuss future work and potential improvements.

II. STANDARD PREDICTIVE CONTROL APPROACH

Model Predictive Control (MPC) has been a popular approach for industrial control systems [7]. The MPC problem involves optimizing a cost function subject to the dynamics of the system, over a finite horizon of time. The first computed input is applied, and at the next step the optimization is solved again. With predictions for future load, it is possible to develop a optimization formulation to minimize the peak power demand on the energy storage component of a HES. For example, Choi et al. [8] applied finite-horizon control to a battery-supercapacitor system with linear capacitor (energy storage) dynamics and a log-barrier cost function to smooth the battery (power source) current profile over a time-varying load demand. This resulted in a continuous control of both

the battery and the capacitor together, but required exact knowledge of the future demand of load.

Even with perfect predictions of the load demand, optimization horizons cannot be arbitrarily long. With this in mind, we can apply existing control techniques like MPC to control the HES with a norm cost on the power supplied from the power source. Eq. (2) shows the MPC formulation for a HES with discretized dynamics and upper and lower energy storage limits on the power storage. Note, the power source is treated as an infinite energy source but has a high cost of use while the energy storage has limited energy capacity but has no cost of use.

$$\text{minimize } \|\mathbf{u}\|_p \quad (2a)$$

$$\text{subject to} \quad (2b)$$

$$u(t+i) + v(t+i) = d(t+i), \quad (2c)$$

$$x(t+i+1) = x(t+i) - hv(t+i), \quad (2d)$$

$$x_{\min} \leq x(t+i) \leq x_{\max}, \quad \forall i = 0, \dots, M \quad (2e)$$

Here, Eqs. (2c) and (2d) hold $\forall i = 0, \dots, M-1$, where M is the control horizon, h is the sampling time, and $\mathbf{u} = [u(t), \dots, u(t+M-1)]^T$. Eq. (2c) is the balance equation (1). Eq. (2d) is the discretized energy dynamics of the energy storage (discretization period is h), and we assume there is no loss term, although linear loss terms can be easily incorporated. Finally, Eq. (2e) implies that the SoC of the energy source, x , has to be within some bounds at all times.

A. Limitations of standard MPC

While MPC is a logical formulation for peak minimization in HES, there are some drawbacks to using MPC:

- 1) MPC needs fine-grained information about the load demand, i.e., either the exact load demand, or its distribution (for stochastic MPC), at every time instant, which is difficult to obtain for many practical systems.
- 2) For a system with fast dynamics, the computational requirements for MPC may make it impractical for implementation, especially given limited computational capability. Move-blocking MPC [9] has been developed as a technique to reduce the computational overhead by reducing the number of control variables to be solved for. However it assumes a constant control signal during each blocking window, which consists of multiple time steps. This may result in infeasibility given some constraints on the system's state variables, e.g., x in Eq. (2e) may violate its upper or lower limits if the control signal is not free to change at every time step.

III. MULTI-LEVEL CONTROL APPROACH

To overcome the aforementioned drawbacks of move-blocking MPC we propose a multi-level control approach based on the following fundamental idea. Consider the load curve from the current time t_0 to some time instant $t_f > t_0$ as depicted by the solid line in Fig. 2. The interval $[t_0, t_f]$ is divided into $N \geq 1$ equidistant subintervals: $t_0 < t_1 < \dots < t_N = t_f$. During each $[t_i, t_{i+1})$, $0 \leq i \leq N-1$, we set a peak threshold \bar{P}_i on u and control the source and the storage so that u does not exceed \bar{P}_i at any time during the

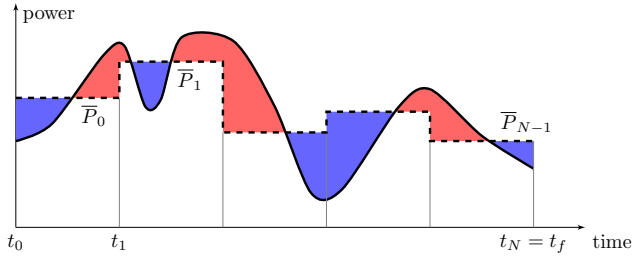


Fig. 2. The fundamental idea of the proposed control approach.

subinterval, i.e., $u(t) \leq \bar{P}_i, \forall t \in [t_i, t_{i+1})$. In Fig. 2, the peak thresholds for the subintervals are illustrated by the dashed lines. The residuals between the load and the source will be picked up by the storage. In particular, in Fig. 2, the blue regions when the source power exceeds the load are charged to the storage, while the red regions when the load exceeds the source power are supplied by the storage.

To realize the above idea, we design a control structure consisting of two levels, as illustrated in Fig. 3:

- **High-level control** determines the peak threshold for each time subinterval such that:
 - a global objective is attained, for example the overall peak of u is reduced, and
 - each individual peak threshold can be satisfied while ensuring that the instantaneous load is provided.
- **Low-level control** determines, at any time t , the powers $u(t)$ and $v(t)$ so that the required load is served, the peak threshold for the current subinterval (as determined by the high-level control) is satisfied, and the storage is neither over-charged or over-exhausted.

The two control levels are linked by the peak thresholds \bar{P}_i , which are computed by the high-level control and executed by the low-level control.

A. Low-level Control

Let $\bar{P}(t)$ denote the peak threshold in effect at time t , i.e., $\bar{P}(t) = \bar{P}_i$ if $t \in [t_i, t_{i+1})$. The general rule for the low-level control is to keep u at the peak threshold for the current subinterval as long as it is feasible to do so.

- If the storage is not exhausted ($x(t) > x_{\min}$) and the load exceeds the peak threshold ($d(t) > \bar{P}(t)$), the storage is discharged to supply for the residual.
- If the storage is not fully charged ($x(t) < x_{\max}$) and the peak threshold exceeds the load ($d(t) < \bar{P}(t)$), we keep $u(t) = \bar{P}(t)$ to charge the storage with the surplus energy, so that should the demand spike later on, the stored energy can be used to alleviate the peak.

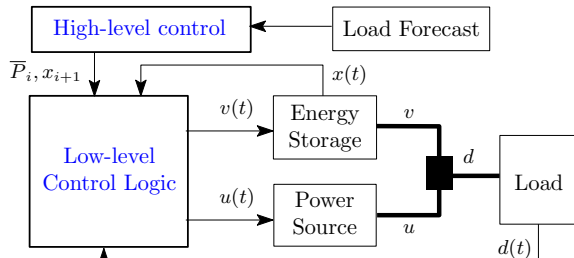


Fig. 3. Structure of the proposed control approach.

If this rule is infeasible then the source must track the load, i.e., $u(t) = d(t)$. Specifically, the low-level control logic is described in Alg. 1, where we omit the time t for brevity.

A *top saturation* is an interval $[t_1, t_2]$ during which the storage is saturated at the maximum SoC x_{\max} , i.e., $x(t) = x_{\max}$ and $d(t) < \bar{P}(t) \forall t \in [t_1, t_2]$. Similarly, a *bottom saturation* is an interval $[t_1, t_2]$ during which the storage is saturated at the minimum SoC x_{\min} , i.e., $x(t) = x_{\min}$ and $d(t) > \bar{P}(t) \forall t \in [t_1, t_2]$. These cases correspond to line 4 in Alg. 1. If no saturation happens at time t , the system is *saturation-free*. This case corresponds to line 2 in Alg. 1.

Algorithm 1 Low-level control logic.

```

1: if  $(d \leq \bar{P} \wedge x < x_{\max}) \vee (d \geq \bar{P} \wedge x > x_{\min})$  then
2:    $u \leftarrow \bar{P}, v \leftarrow d - \bar{P}$ 
3: else
4:    $u \leftarrow d, v \leftarrow 0$ 
5: end if

```

B. Interface Between High and Low Control Levels

The key result of this paper, presented in Theorem 1, regards the interface between the high-level control and the low-level control. It specifies a sufficient condition on the peak thresholds \bar{P}_i , as computed by the high-level control, so that with the low-level control logic in Alg. 1 the set peak thresholds are always honored. Let the notation d^+ denote the non-negative portion of the load's demand, i.e., $d^+(t) = d(t)$ if $d(t) \geq 0$ and $d^+(t) = 0$ otherwise.

Theorem 1: Given an interval $[0, T]$, $T > 0$, a desired final SoC $x_f \in [x_{\min}, x_{\max}]$, and E^+, E, \bar{d} such that

$$E^+ \geq \int_0^T d^+(t) dt \geq 0 \quad (3a)$$

$$E \geq \int_0^T d(t) dt \quad (3b)$$

$$\bar{d} \geq \max_{0 \leq t < T} d(t). \quad (3c)$$

Choose any peak threshold $\bar{P} \geq 0$ satisfying

$$\bar{P} \geq (x_f - x(0) + E) / T \quad (4)$$

and, if $E^+ > 0$,

$$\bar{P} \geq \bar{d} (1 - (x(0) - x_{\min}) / E^+), \quad (5)$$

$$\bar{P} \geq \bar{d} (1 - (x_{\max} - x_f) / E^+). \quad (6)$$

Then with the low-level control algorithm in Alg. 1, the following statements hold:

a) For all $t \in [0, T]$: $u(t) \leq \bar{P}$.

b) $x(T) \geq x_f$.

Statement (a) essentially confirms that, with the chosen peak threshold \bar{P} , the source power never exceeds the peak threshold. Furthermore, by statement (b), the final SoC of the storage is at least x_f (i.e., the desired final SoC is achieved). The proof of Theorem 1 can be found in the Appendix.

IV. HIGH-LEVEL CONTROL

The key result in Theorem 1 connects the high-level control and the low-level control. Essentially, to ensure that the peak threshold set by the high-level control is always honored by the low-level control, it should satisfy the sufficient conditions

given in the Theorem. In this section, we formulate the high-level control problem using a receding-horizon control (RHC) approach [7].

Let us recall the fundamental idea of our approach in Section III. We divide a given time horizon $[t_0, t_f]$ into N subintervals. In the high-level control, we determine for each subinterval i a peak threshold \bar{P}_i , which is then used by the low-level control in Alg. 1. The computed peak thresholds are good if they not only satisfy the sufficient conditions in Theorem 1 but also optimize a certain global objective for the horizon $[t_0, t_f]$. The latter can be represented in a RHC formulation. In the next subsection, we discuss the load forecast information required by the high-level control to compute the peak thresholds.

A. Required Load Forecast Information

From Theorem 1, to determine a peak threshold for each subinterval $[t_i, t_{i+1})$, $0 \leq i \leq N-1$, the high-level control requires the three values defined in Eq. (3), namely

- $E_i^+ \geq \int_{t_i}^{t_{i+1}} d^+(t) dt$ is an upper bound of the total non-negative energy demand for the subinterval;
- $E_i \geq \int_{t_i}^{t_{i+1}} d(t) dt$ is an upper bound of the total net energy demand for the subinterval;
- $\bar{d}_i \geq \max_{t_i \leq t < t_{i+1}} d(t)$ is an upper bound of the maximum power demand during the subinterval.

Note that E_i^+ , E_i and \bar{d}_i are upper-bound estimates of the corresponding values on the right-hand side, so exact estimates of these values are preferred but not required. To obtain these estimates for each time subinterval requires a prediction of the load during the subinterval. Depending on the actual application, the level of technical effort involved in the prediction might vary widely. For example, if the load is generated by electric appliances in a building, the upper bound estimates can be calculated based on the schedule or the history of appliance use, which is relatively easy. However, if the load is generated by the motors of an EV, obtaining these estimates will be much more difficult as it involves predicting the road condition, the traffic condition, and the driving habits to name a few. For that reason, we assume that these estimates are available and ignore for now the technical details of obtaining them.

B. High-level Control Optimization

Given a horizon $[t_0, t_f]$ divided into N subintervals, the high-level control determines the peak thresholds such that the conditions in Theorem 1 are satisfied and a global objective function $F(\mathbf{P})$ is minimized. Here \mathbf{P} is the vector of the peak thresholds: $\mathbf{P} = [\bar{P}_0, \dots, \bar{P}_{N-1}]^T$. The choice of the objective function depends on the goals of the application. A possible choice is the l_p -norm function $F(\mathbf{P}) = \|\mathbf{P}\|_p$, where $\|\cdot\|_p$ denotes the l_p -norm of a vector, for $p \geq 1$ or $p = \infty$. When the l_∞ -norm is used, the overall peak during $[t_0, t_f]$ is minimized because $\|\mathbf{P}\|_\infty = \max_{0 \leq i \leq N-1} \bar{P}_i$. In our case study in Section VI we found that the l_2 -norm worked best to both smoothen the u curve and reduce its overall peak. To further smoothen u we can penalize the variations in \mathbf{P} by adding a term $\sum_{i=0}^{N-2} |\bar{P}_{i+1} - \bar{P}_i|$. For

example $F(\mathbf{P}) = \|\mathbf{P}\|_p + \epsilon \sum_{i=0}^{N-2} |\bar{P}_{i+1} - \bar{P}_i|$ where $\epsilon > 0$ is a predefined constant.

Let x_i , $1 \leq i \leq N$, be the desired SoC of the storage at the end of the subinterval $[t_i, t_{i+1}]$. These values are also determined by the high-level control. The final desired SoC x_N can be either free or fixed at a predefined value $x_f \in [x_{\min}, x_{\max}]$. We can now formulate the high-level control optimization for the interval $[t_0, t_f]$ as follows:

$$\text{minimize}_{\mathbf{P}, x_1, \dots, x_N} F(\mathbf{P})$$

subject to

$$\bar{P}_i \geq (x_{i+1} - x_i + E_i) / (t_{i+1} - t_i) \quad (7a)$$

$$\text{if } E_i^+ > 0: \bar{P}_i \geq \bar{d}_i (1 - (x_i - x_{\min}) / E_i^+) \quad (7b)$$

$$\text{if } E_i^+ > 0: \bar{P}_i \geq \bar{d}_i (1 - (x_{\max} - x_{i+1}) / E_i^+) \quad (7c)$$

$$\bar{P}_i \geq 0 \quad (7d)$$

$$x_{\min} \leq x_{i+1} \leq x_{\max} \quad (7e)$$

$$x_0 = x(t_0), \quad x_N = x_f \quad (7f)$$

in which the constraints (7a) to (7e) are satisfied for all $i = 0, \dots, N-1$. Eq. (7e) constraints the SoC between x_{\min} and x_{\max} . Eq. (7f) specifies the initial condition and the (optional) final condition on the SoC of the storage. We remark that all the constraints are linear, therefore if F is convex the optimization (7) can be solved efficiently [10].

C. Receding-Horizon High-level Control Algorithm

The optimization (7) only solves the peak thresholds for a finite time horizon, which is usually due to the limitation that we cannot predict the load too far into the future. However, the system typically operates far beyond that time horizon, possibly forever. In order to compute the peak thresholds continuously as time progresses, we employ the *receding-horizon control* approach [7].

Let $T_s > 0$ be the sampling time step and $t_i = iT_s$, $i \in \mathbb{N}$, be the sampling instants of the high-level control. We assume that at each t_i we can obtain the predictions (E_j^+, E_j, \bar{d}_j) for N future steps: $i \leq j \leq i + N - 1$. The RHC approach is illustrated in Fig. 4. At time t_i , we solve Eq. (7) for the time window $[t_i, t_{i+N}]$ consisting of N sampling intervals. We then apply the resulting optimal peak thresholds and desired SoCs for only the first interval $[t_i, t_{i+1}]$. At the next time instant t_{i+1} , the N -step horizon window is advanced by one step to $[t_{i+1}, t_{i+1+N}]$, for which new predictions are obtained and the optimization process is repeated. The high-level control algorithm is summarized in Alg. 2.

Algorithm 2 RH high-level control algorithm.

```

for  $i = 0, 1, 2, \dots$  do
  Obtain  $(E_j^+, E_j, \bar{d}_j)$  for  $j = i, \dots, i + N - 1$ 
  Solve optimization (7)
  Apply  $\bar{P}_i$  and  $x_{i+1}$ 
  Wait until  $t_{i+1}$ 
end for

```

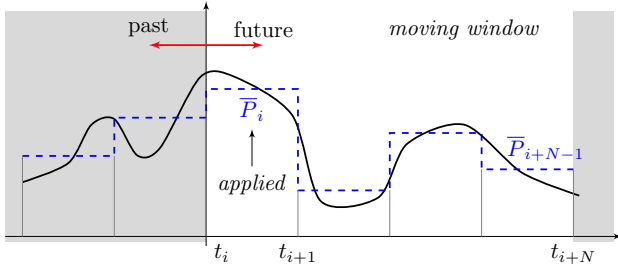


Fig. 4. RHC approach for high-level control: The solid line is the load. The dashed line is the peak threshold determined by the high-level control. Optimization (7) is solved for a moving time window of N sampling steps.

D. Adaptive Peak Threshold

The low-level control algorithm uses a constant peak threshold \bar{P}_i throughout the interval $[t_i, t_{i+1}]$. The calculation of \bar{P}_i by the high-level control is often over-conservative due to our lack of knowledge of the actual future load during the interval. However, as time progresses, at time $t \in [t_i, t_{i+1}]$, we have knowledge of the past load from t_i to t , hence we can improve the peak threshold to be less conservative. In other words, we can adapt the peak threshold with the feedback information from the past load. Specifically, define $\mathcal{E}_i(t) = E_i - \int_{t_i}^t d(\tau) d\tau$ and $\mathcal{E}_i^+(t) = E_i^+ - \int_{t_i}^t d^+(\tau) d\tau$, which can be calculated by simple integrators. Note that $\mathcal{E}_i(t_i) = E_i$ and $\mathcal{E}_i^+(t_i) = E_i^+$. Then, by considering $[t, t_{i+1}]$ as the time interval in Theorem 1, we can re-compute the peak threshold for the rest of the interval, as in Alg. 3. The adaptive peak threshold computation is executed periodically after every $T_a > 0$ time units during each interval $[t_i, t_{i+1}]$.

Algorithm 3 Adaptive peak threshold algorithm.

```

repeat every instant  $t = t_i, t_i + T_a, \dots$  during  $[t_i, t_{i+1}]$ 
  Obtain  $\mathcal{E}_i(t)$  and  $\mathcal{E}_i^+(t)$ 
   $\bar{P} \leftarrow \max\{0, (x_{i+1} - x(t) + \mathcal{E}_i(t)) / (t_{i+1} - t)\}$ 
  if  $\mathcal{E}_i^+(t) > 0$  then
     $\bar{P} \leftarrow \max\{\bar{P}, \bar{d}_i (1 - (x(t) - x_{\min}) / \mathcal{E}_i^+(t)),$ 
       $\bar{d}_i (1 - (x_{\max} - x_{i+1}) / \mathcal{E}_i^+(t))\}$ 
  end if
end repeat

```

It can be shown, using Lemma 1 in the Appendix, that for all $t_i \leq t < t' \leq t_{i+1}$, if $\mathcal{E}_i^+(t) > 0$ and $\mathcal{E}_i^+(t') > 0$ then $\bar{d}_i \left(1 - \frac{x(t) - x_{\min}}{\mathcal{E}_i^+(t)}\right) \geq \bar{d}_i \left(1 - \frac{x(t') - x_{\min}}{\mathcal{E}_i^+(t')}\right)$. Hence, the lower-bound on \bar{P} in Eq. (5) is non-increasing during the interval. Similarly, we can show that the lower-bounds on \bar{P} in Eqs. (4) and (6) are also non-increasing. Therefore, it is guaranteed that the adjusted peak threshold computed by Alg. 3 will not increase towards the end of the interval.

V. OVERALL CONTROL STRUCTURE

We have discussed in Sections III to IV the essential components of the proposed control scheme: the *low-level control*, the *high-level control* and the *adaptive peak threshold algorithm*. These components are put together in the overall control structure in Fig. 5. At the bottom right is the plant consisting of the power source, the energy storage and the load. At the top is the *high-level control* which carries out load forecasting and the receding-horizon control algorithm

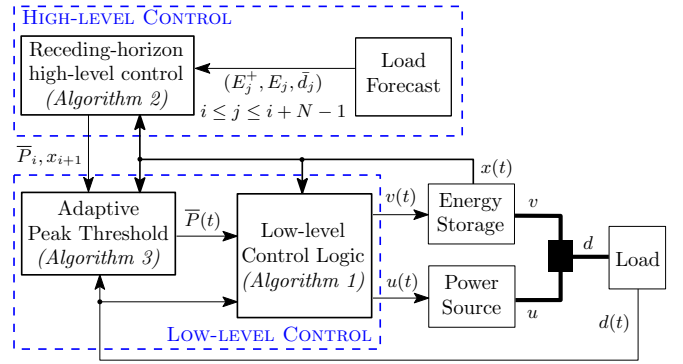


Fig. 5. Overall detailed structure of the proposed scheme.

(Alg. 2). The calculated peak thresholds and desired SoCs are then provided to the *low-level control*. The *adaptive peak threshold* algorithm (Alg. 3) periodically adjusts the peak constrain $\bar{P}(t)$, which is used by the low-level control algorithm (Alg. 1) to control the powers of the source and the energy storage.

Fig. 5 highlights an important feature of the proposed scheme, that is the separation between the executions of the high-level control and the low-level control. In particular:

- The low-level control consists of simple algorithms. Therefore its implementation is simple and it can be executed at a very fast rate.
- The high-level control, which consists of more complex algorithms involving load predictions and an optimization, can be executed at a much slower rate.

An implication of this feature is that any change in the execution (sampling) rate of the low-level control does not affect the high-level control. This helps reduce the development and implementation cost of the control scheme.

VI. CASE STUDY : POWER MANAGEMENT IN ELECTRIC VEHICLES

To demonstrate the proposed scheme we consider the case of an EV with a battery and supercapacitor (SC) HES. A battery has a relatively high energy density but a low power density compared to an SC. The low power density results in the following problems: (a) a large number of battery packs are needed to provide sufficient peak power to the electrical systems, and (b) the battery life can be diminished through large variations of current flow that generate excessive heat and increase the internal resistance of the battery [2]. In contrast, the SC has a relatively high power density but a low energy density compared to the battery.

Keeping the battery operating temperature under check is necessary to avoid battery degradation. Modular designs of the battery have been used to explore partitioning and control of individual or a group of cells [11] for thermal management. The use of SCs to reduce the power drawn from the battery has also been explored extensively. Rule based and non-predictive control of battery supercapacitor systems has been studied in [12], [13]. Predictive control for such systems has also been studied with finite horizon control involving perfect knowledge of future load demand [8] and also with data-driven model predictive control [14]. For the

scope of this study, we obtain predictions from historic data. This is covered in more detail in section VI-B. Note that the scheme proposed in this paper does not need exact prediction of load demand at every time instant (cf. Section IV).

A. Peak power reduction for EV batteries

Reducing the peak power drawn from the battery has a direct impact on the battery's thermal behavior. Battery thermal models [15], [16] show that the battery module's rate of change of temperature increases with both charging and discharging. Simplified thermal dynamics of the battery can be obtained from the energy balance equation [15] as $K \frac{dT}{dt} = Q + H$ where K is a constant. Here the rate of temperature change $\frac{dT}{dt}$ is proportional to the heat H due to convection and the heat Q due to power flow in and out of the battery. Q is directly proportional to the power $I^2 R_{int}$ where I is the battery current and R_{int} is the battery's internal resistance. SCs, with their low-energy storage and high charge/discharge rate capacities [6], can be used to partially or completely meet the peak power demands from the load (for a short period of time), effectively reducing the power drawn from the battery and hence reducing heat generation in the battery. Figure 1 shows a general architecture for a battery supercapacitor energy source delivering power to a motor. Details on the architecture can be found in [6].

B. Generating predictions for the proposed scheme

In order to get predictions of the load demand parameters of Theorem 1, we rely on historical data. For the simulations in this paper, we use data from the ChargeCar project [17] to give us real world drive cycles and also to predict the required parameters. To get predictions for our scheme and Stochastic MPC, we limit ourselves to trips along a particular route (assumed that the route is known *a priori*). This is done to reduce the amount of data to be processed and also since intuitively, the driving profile is expected to be similar for trips along a particular route. Figure 6 shows the route along which the simulation trips are. It is a 1.1 mile trip, and for driver data we used, the fastest trip took 16 minutes, the longest 19.4 minutes and on an average it took 17.5 minutes to complete the trip. To average simulation data across all trips, we truncated all trips to 16 minutes. Since there is limited data for trips along the same route (9 trips along the route selected for simulations in the paper), we take all the trips to generate the predictions (worst case upper bounds for parameters needed for the proposed scheme and maximum likelihood estimation for the stochastic MPC) and then pick one of the trips as the simulation trip. While this follows the unagreeable practice of having a testing set which is a subset of the training set, this is necessary to make the parameters $E, E+, \bar{d}$ be upper bounded by the worst case for all trips. Since the focus of this paper is on the control algorithm of the proposed scheme itself, the development of more advanced prediction schemes is left for future work.

C. Control schemes for the battery supercapacitor system

In order to show the effectiveness of the proposed scheme in reducing peak power drawn from the battery (and hence

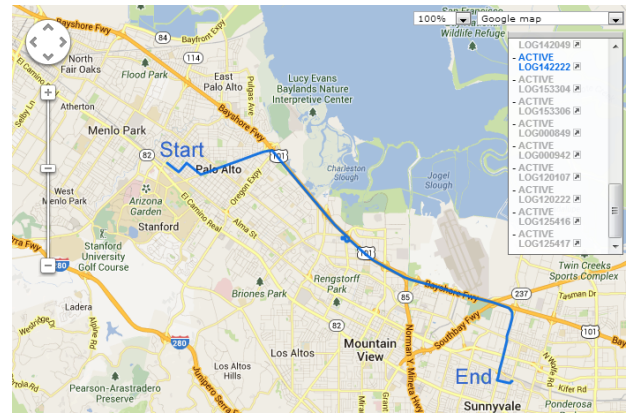


Fig. 6. GPS coordinates for the selected simulation.

reducing battery temperature) we implemented and evaluated the following schemes for comparison:

- 1) **Battery-only:** The load demand is met by the battery only. This serves as a worst-case reference (for any scheme with a supercapacitor).
- 2) **Naive scheduling:** This scheme uses the SC to meet the load whenever it has charge, and charges the SC with regeneration (if the SC is not already at maximum storage capacity).
- 3) **Stochastic MPC:** Since the future load demand being known perfectly is nearly impossible for an EV, we modify the MPC formulation in Eq. (2) to take in a load vector \mathbf{d} in the form of a multivariate normal distribution. This distribution is obtained by taking historic data and fitting a multivariate distribution using maximum likelihood estimation and the constraints involving are now stochastic, to be met with a high probability. Due to limited space we do not elaborate upon the formulation, but details on stochastic MPC formulations can be found in [18].
- 4) **Optimal scheme:** The optimal control formulation is similar to the deterministic MPC formulation in Eq. (2), except that the horizon M is the length of the entire simulation. The optimization is solved in one shot, and is done offline.

Note that the optimal scheme gives the best-case performance (since the optimization is done with load demand known perfectly *a priori*) which we use as a baseline to evaluate any scheme. In practice, this optimal scheme is intractable for lengthy drive cycles because the entire driving period has to be known *a priori*.

The proposed control scheme needs comparatively less information than stochastic MPC and the optimal scheme: only the upper bounds on the total energy demanded by the load and the maximum power demand in the horizon. Also, due to the separation of the two control levels, the high-level optimization can be solved at a low rate, irrespective of the sampling rate for the low-level control. These features make the scheme attractive in practice.

D. Simulation setup

To evaluate the effectiveness of the proposed scheme and the battery supercapacitor control schemes outlined above, we use the Advanced Vehicle Simulator (ADVISOR) developed by National Renewable Energy Lab (NREL) [19]. The schemes are evaluated with the load power demand generated

for an EV going through drive cycles on the route chosen from the ChargeCar data. We use the Lithium-Ion battery model in ADVISOR and simulate it for the battery power profile generated for the real world drive cycles by the different schemes. The temperature and SoC profiles generated from the simulation are used to compare the performance of the different schemes.

E. Simulation results

We simulated our scheme and the others for all the nine trips on the same route with the SC half full initially. The SC has ratings of 50F and 60V. The ADVISOR Li-ion battery consists of 25 12V-cells rated at 7.035Ah (at C/3 discharge rate and 25 °C). For our scheme we used $N = 8$, $T_s = 5$ s and $T_a = 1$ s. For the stochastic MPC, the horizon was limited to 8 s since maximum likelihood estimation can fit only a distribution of length less than or equal to the number of data sets available (9 trips at 1Hz sampling in our case). The proposed scheme and stochastic MPC used a l_2 -norm cost function for the optimizations (solved with YALMIP). The simulations were carried out on a Intel i5 machine (2.5GHz, 6GB RAM) running MATLAB R2012a.

Figure 7 shows the mean temperature profiles for a Li-Ion battery subject to the 9 drive cycle from ChargeCar data and controlled by the different schemes. The simulation results for all schemes are summarized in Table I, which presents the relevant battery parameters, averaged over the 9 simulation trips. Observe that our scheme performs as well as stochastic MPC and leads to a marked reduction in the average and the maximum battery temperatures compared to the battery-only and the naive schemes. These results show the effectiveness of the proposed scheme in reducing the battery operating temperature, with only historic data. The naive scheme has very little improvement over the battery-only scheme. This implies that using initial charge in the capacitor and regenerative energy alone to charge the SC does not give the best possible use of the SC.

In terms of computation time, for a drive cycle length of 965s and at 1Hz sampling rate, stochastic MPC took an average of 579s while our scheme took significantly less time, only 29s on average. This is because the stochastic MPC implementation repeats its optimization at every time step of 1s, while our scheme only needs to solve the high-level optimization every 5s. The computation time of the low-level control is negligible due to its simplicity. Moreover, because of the separation of the two control levels in our scheme, increasing the low-level sampling rate of the system does not affect the computation time of the high-level control.

VII. CONCLUSION

In this paper, we developed a multi-level control scheme for peak power reduction in HES. The basic idea is to cap the power drawn from the source by a peak threshold while using the energy storage for the residual between the load and the source power. We provided a sufficient condition for the peak threshold calculated by the high-level control to be feasible for the low-level control logic. This architecture allows the complex computations be decoupled from the

Scheme	MaxTemp (C)(%)	MeanTemp (C)(%)	Exec. Time (s)
Proposed scheme	47.1733 (9.57)	27.5373 (6.24)	29.50
Stochastic MPC	47.3732 (9.18)	28.0696 (4.43)	579.29
Optimal	38.5115 (26.16)	24.6182 (16.15)	0.49
Naive	50.6186 (2.96)	28.9097 (1.57)	N/A
Battery-only	52.1639	29.3711	N/A

TABLE I

BATTERY PARAMETERS (AVERAGED OVER THE TRIPS USED FOR

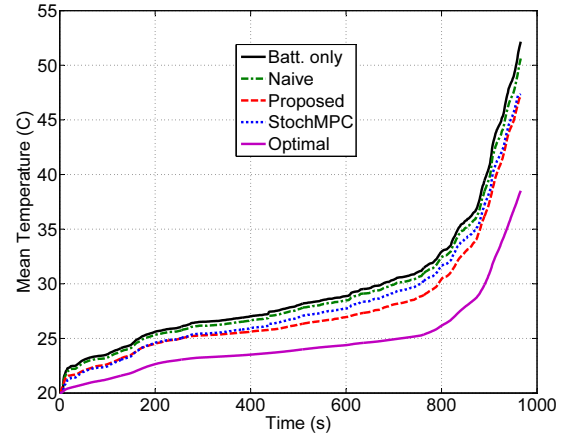


Fig. 7. Battery temperature (averaged over all simulation trips) vs time for different schemes. A lower battery temperature increases battery lifetime.

low-level sampling rate, hence making the proposed scheme efficient computationally and applicable to systems with fast dynamics. A notable advantage of this scheme is that it does not require exact and fine grained predictions of the load at every time step. Using a case study of a battery and supercapacitor energy system for electric vehicles, we evaluated the proposed scheme and showed its effectiveness in reducing peak battery power (hence battery temperature) as well as its applicability to fast dynamical systems.

REFERENCES

- [1] M. H. Albadi and E. F. El-Saadany, "Demand response in electricity markets: An overview," in *Proc. IEEE Power Engineering Society General Meeting*, 2007, pp. 1–5.
- [2] Wikipedia, "Battery life (and death)," <http://www.mpoweruk.com/life.htm>, accessed: 2013-04-09.
- [3] National Geographic, "Upgrading the electric grid with flywheels and air," <http://news.nationalgeographic.com/news/energy/2011/2/110223-electric-grid-flywheels-compressed-air.html>, accessed: 2013-04-12.
- [4] Y. Ma, F. Borrelli, B. Hency, B. Coffey, S. Bengea, and P. Haves, "Model predictive control for the operation of building cooling systems," in *Proceedings of the American Control Conference*, 2010.
- [5] J. Liu, P. H. Chou, N. Bagherzadeh, and F. Kurdahi, "Power-aware scheduling under timing constraints for mission-critical embedded systems," in *Proc. Design Automation Conference*. ACM, 2001.
- [6] A. Khaligh and Z. Li, "Battery, ultracapacitor, fuel cell, and hybrid energy storage systems for electric, hybrid electric, fuel cell and plug-in hybrid electric vehicles: State of the art," *IEEE Tran. on Vehicular Tech.*, 2008.
- [7] E. Camacho and C. Bordons, *Model predictive control*. Springer Verlag, 2004.
- [8] M. Choi, S. Kim, and S. Seo, "Energy management optimization in a battery/supercapacitor hybrid energy storage system," *IEEE Transactions on Smart Grid*, 2012.
- [9] R. Cagienard, P. Grieder, E. Kerrigan, and M. Morari, "Move blocking strategies in receding horizon control," *IEEE CDC*, 2004.
- [10] S. Boyd and L. Vandenberghe, *Convex Optimization*. Cambridge University Press, 2006.

- [11] H. Kim and K. Shin, "Scheduling of battery charge, discharge, and rest," *Proc. IEEE Real-Time Systems Symposium*, 2009.
- [12] R. Carter and A. Cruden, "Strategies for control of a battery/supercapacitor system in an electric vehicle," *Intl. Symp. on Power Electronics, Electrical Drives, Automation and Motion*, 2008.
- [13] J. Awerbuch and C. Sullivan, "Control of ultracapacitor-battery hybrid power source for vehicular applications," *IEEE Conf. on Global Sust. Energy Infrastructure: Energy2030*, 2008.
- [14] A. Styler and I. Nourbakhsh, "Model predictive control with uncertainty in human driven systems," *AAAI Conf. on Artif. Intelligence*, 2013.
- [15] A. Pesaran, A. Vlahinos, and S. Burch, "Thermal performance of ev and hev battery modules and packs," *Proceedings of the 14th International Electric Vehicle Symposium*, 1997.
- [16] M. Zahrand and A. Atef, "Electrical and thermal properties of ncd battery for low earth orbit satellite's applications," *Proceedings of the 6th WSEAS International Conference on Power Systems*, 2006.
- [17] ChargeCar, <http://www.chargecar.org>, accessed: 2013-09-23.
- [18] F. Oldewurtel, C. Jones, and M. Morari, "A tractable approximation of chance constrained stochastic mpc based on affine disturbance feedback," *IEEE Conf. on Dec. and Control*, 2008.
- [19] K. Wipke, M. Cuddy, D. Bharathan, S. Burch, V. Johnson, A. Markel, and S. Sprik, "Advisor 2.0: A secondgeneration advanced vehicle simulator for systems analysis," NREL, Tech. Rep., March 1999.

APPENDIX: PROOF OF THEOREM 1

To prove Theorem 1 we need the following Lemma.

Lemma 1: Define function $\mathcal{E}^+(t) = E^+ - \int_0^t d^+(\tau) d\tau$. Then for all $0 \leq t < t' \leq T$,

$$\mathcal{E}^+(t')(x(t) - x_{\min}) \leq \mathcal{E}^+(t)(x(t') - x_{\min}). \quad (8)$$

Proof: By the definition of \mathcal{E}^+ , we have $\mathcal{E}^+(t) \geq \mathcal{E}^+(t') \geq 0$. If $x(t) \leq x(t')$ then obviously Eq. (8) holds, so we assume that $x(t) > x(t')$. Similarly, if $\mathcal{E}^+(t) = 0$ or $\mathcal{E}^+(t') = 0$ then Eq. (8) trivially holds. Therefore we also assume that $\mathcal{E}^+(t) > 0$ and $\mathcal{E}^+(t') > 0$, thus $E^+ > 0$ and Eq. (5) holds. Furthermore, we suppose that

$$\bar{P} \geq \bar{d} \left(1 - \frac{x(t) - x_{\min}}{\mathcal{E}^+(t)} \right), \quad (9)$$

which will be justified later. To prove Eq. (8), we first consider the basic case when there is no saturation between t and t' .

Basic case. Let $\Delta_t = t' - t$, $\Delta_E^{\max} = \bar{d}\Delta_t \geq \Delta_E^+$, $\Delta_E = \int_t^{t'} d(\tau) d\tau$, $\Delta_E^+ = \mathcal{E}^+(t) - \mathcal{E}^+(t') = \int_t^{t'} d^+(\tau) d\tau \geq \Delta_E$. Because there is no saturation between t and t' , $u(t) = \bar{P} \forall t \leq t \leq t'$. Therefore $x(t') = x(t) - \int_t^{t'} (d(\tau) - \bar{P}) d\tau = x(t) + \bar{P}\Delta_t - \Delta_E$. Since $x(t) > x(t')$ we have $\Delta_E^{\max} \geq \Delta_E^+ \geq \Delta_E > \bar{P}\Delta_t \geq 0$ and $\bar{d} > 0$. We want to show that

$$\frac{x(t) - x(t')}{\mathcal{E}^+(t) - \mathcal{E}^+(t')} = \frac{\Delta_E - \bar{P}\Delta_t}{\Delta_E^+} \leq \frac{x(t) - x_{\min}}{\mathcal{E}^+(t)}. \quad (10)$$

Indeed, if $\frac{x(t) - x_{\min}}{\mathcal{E}^+(t)} \geq 1$ then Eq. (10) clearly holds because $\frac{\Delta_E - \bar{P}\Delta_t}{\Delta_E^+} \leq 1$. Consider the case when $\frac{x(t) - x_{\min}}{\mathcal{E}^+(t)} < 1$. Multiplying inequality (9) with $\Delta_t > 0$ we have $\bar{P}\Delta_t \geq \Delta_E^{\max} \left(1 - \frac{x(t) - x_{\min}}{\mathcal{E}^+(t)} \right)$. Therefore

$$\frac{\Delta_E - \bar{P}\Delta_t}{\Delta_E^+} \leq \left[\Delta_E - \Delta_E^{\max} \left(1 - \frac{x(t) - x_{\min}}{\mathcal{E}^+(t)} \right) \right] / \Delta_E^+. \quad (11)$$

On the other hand, multiplying the inequality $\frac{x(t) - x_{\min}}{\mathcal{E}^+(t)} < 1$ with $(\Delta_E^+ - \Delta_E^{\max}) \leq 0$ gives us $\frac{x(t) - x_{\min}}{\mathcal{E}^+(t)} (\Delta_E^+ - \Delta_E^{\max}) > \Delta_E^+ - \Delta_E^{\max} \geq \Delta_E - \Delta_E^{\max}$ where the last inequality comes from $\Delta_E^+ \geq \Delta_E$. Expanding the above inequality we get

$$\frac{x(t) - x_{\min}}{\mathcal{E}^+(t)} > \left[\Delta_E - \Delta_E^{\max} \left(1 - \frac{x(t) - x_{\min}}{\mathcal{E}^+(t)} \right) \right] / \Delta_E^+. \quad (12)$$

Then Eq. (10) follows from Eqs. (11) and (12). Now that we have shown Eq. (10), we cross-multiply it to obtain

$$\mathcal{E}^+(t)(x(t) - x(t')) \leq (\mathcal{E}^+(t) - \mathcal{E}^+(t'))(x(t) - x_{\min})$$

which is simplified to Eq. (8). The basic case is complete.

General case. In the general case, when there might be saturations between t and t' , we can always divide the interval $[t, t']$ into $k \geq 1$ consecutive subintervals

$$[t, t'] = [t^{(0)}, t^{(1)}] \cup [t^{(1)}, t^{(2)}] \cup \dots \cup [t^{(k-1)}, t^{(k)}]$$

where $t = t^{(0)} < t^{(1)} < \dots < t^{(k)} = t'$, such that during each entire subinterval, the system is either saturated or saturation-free. Consider any subinterval $[t^{(i)}, t^{(i+1)}]$, $0 \leq i \leq k - 1$. During the subinterval, if the system is saturated then $x(t^{(i)}) = x(t^{(i+1)})$, hence Eq. (8) holds. On the other hand, if the system is saturation-free during the subinterval then Eq. (8) for that subinterval is validated by the basic case. In addition, recall that $\mathcal{E}^+(t) > 0$ and $\mathcal{E}^+(t') > 0$, thus $\mathcal{E}^+(t^{(0)}) \geq \dots \geq \mathcal{E}^+(t^{(k)}) > 0$. Therefore we have

$$\frac{x(t^{(0)}) - x_{\min}}{\mathcal{E}^+(t^{(0)})} \leq \frac{x(t^{(1)}) - x_{\min}}{\mathcal{E}^+(t^{(1)})} \leq \dots \leq \frac{x(t^{(k)}) - x_{\min}}{\mathcal{E}^+(t^{(k)})}$$

which verifies Eq. (8) for $[t, t']$.

Proof of Eq. (9). We showed that Eq. (9) implies Eq. (8). We now prove Eq. (9) $\forall t \in [0, T]$ such that $\mathcal{E}^+(t) > 0$. By Eq. (5), Eq. (9) holds for $t = 0$. Consider the interval $[0, t]$ for any $0 < t \leq T$ such that $\mathcal{E}^+(t) > 0$. Then Eq. (8) gives $\frac{x(0) - x_{\min}}{E^+} \leq \frac{x(t) - x_{\min}}{\mathcal{E}^+(t)}$. It follows that $\bar{P} \geq \bar{d}(1 - (x(0) - x_{\min})/E^+) \geq \bar{d}(1 - (x(t) - x_{\min})/\mathcal{E}^+(t))$. Therefore Eq. (9) is verified. ■

A direct consequence of Lemma 1 is the following result.

Lemma 2: There is no bottom saturation during $[0, T]$.

Proof: A bottom saturation happens when $x(t) = x_{\min}$ and $d(t) > \bar{P}$. If $E^+ = 0$ then $d(t) \leq 0 \leq \bar{P}$ for all $t \in [0, T]$. If $E^+ > 0$ then there are two cases. If $x(0) = x_{\min}$ then, by Eq. (5), $\bar{P} \geq \bar{d}$, hence the load can never exceed \bar{P} . The remaining case is when $x(0) > x_{\min}$. Suppose at time $t^* \in [0, T]$, $x(t^*) = x_{\min}$. Then Lemma 1 reads

$$\mathcal{E}^+(t^*)(x(0) - x_{\min}) \leq \mathcal{E}^+(0)(x(t^*) - x_{\min}) = 0.$$

Because $x(0) > x_{\min}$ and $\mathcal{E}^+(t^*) \geq 0$, we must have $\mathcal{E}^+(t^*) = 0$. It follows that $\int_{t^*}^T d^+(t) dt = 0$, that is the load must be non-positive, hence not exceeding \bar{P} , for the rest of the interval. This allows us to conclude. ■

We can now prove Theorem 1.

Proof: Statement (a) follows directly from Lemma 2. For statement (b), there are two cases.

Case 1: during the interval, there is no top saturation.

Then, because there is no bottom saturation either, we have $x(T) = x(0) - \int_0^T (d(t) - \bar{P}) dt = x(0) + \bar{P}T - E$. It follows from Eq. (4) that $x(T) \geq x_f$.

Case 2: there is at least one top saturation during the interval. For this to happen, we must have $E^+ > 0$, hence Eq. (6) holds. Let $t^* \in [0, T]$ be the last time instant of top saturation during the interval, that is $x(t^*) = x_{\max}$ and, if $t^* < T$, $x(t) < x_{\max}$ for all $t^* < t \leq T$. If $t^* = T$ then trivially $x(T) = x_{\max} \geq x_f$. So we only consider $t^* < T$. It

must be that $\bar{d} > \bar{P} \geq 0$ because otherwise, the saturation will continue after t^* . We then have

$$x(T) = x_{\max} + \bar{P}(T - t^*) - \int_{t^*}^T d(t) dt. \quad (13)$$

Let $E^* = \int_{t^*}^T d^+(t) dt$. Obviously $\int_{t^*}^T d(t) dt \leq E^* \leq E^+$ and $E^*/\bar{d} \leq T - t^*$. Then Eq. (13) gives us

$$x(T) \geq x_{\max} + \bar{P} \frac{E^*}{\bar{d}} - E^* = x_{\max} + E^* \left(\frac{\bar{P}}{\bar{d}} - 1 \right).$$

Note that $\bar{P}/\bar{d} - 1 < 0$ because $0 \leq \bar{P} < \bar{d}$. Therefore $x(T) \geq x_{\max} + E^+ (\bar{P}/\bar{d} - 1)$. It then follows from Eq. (6) that $x(T) \geq x_f$. ■